

Lüscher's μ -term and finite volume bootstrap principle for scattering states and form factors

B. Pozsgay¹

¹*Institute for Theoretical Physics
Eötvös University, Budapest
H-1117 Budapest, Pázmány Péter sétány 1/A*

31th March 2008

Abstract

We study the leading order finite size correction (Lüscher's μ -term) associated to moving one-particle states, arbitrary scattering states and finite volume form factors in $1 + 1$ dimensional integrable models. Our method is based on the idea that the μ -term is intimately connected to the inner structure of the particles, ie. their composition under the bootstrap program. We use an appropriate analytic continuation of the Bethe-Yang equations to quantize bound states in finite volume and obtain the leading μ -term (associated to symmetric particle fusions) by calculating the deviations from the predictions of the ordinary Bethe-Yang quantization. Our results are compared to numerical data of the E_8 scattering theory obtained by truncated fermionic space approach. As a by-product it is shown that the bound state quantization does not only yield the correct μ -term, but also provides the sum over a subset of higher order corrections as well.

1 Introduction

The knowledge of the properties of finite volume QFT is of central importance in at least two ways. On one hand, numerical approaches to QFT necessarily deal with a finite volume box and in order to interpret the results correctly a reliable theoretical control of finite size corrections is needed. On the other hand, working in finite volume is not necessarily a disadvantage. On the contrary, the volume dependence of the spectrum can be exploited to obtain (infinite volume) physical quantities like the elastic scattering phase shifts [1, 2] or resonance widths [3, 4].

Finite size mass correction were first derived by Lüscher [5]. The $1 + 1$ dimensional formulas relevant to integrable models together with a generalized F-term formula for moving particles were obtained in [6]. Finite size corrections have recently become important in the context of AdS/CFT correspondence as well. The generalized μ -term and F-term formulas for moving particles with arbitrary dispersion relation were derived in [7, 8].

Besides the volume dependence of the spectrum itself, finite volume form factors (matrix elements of local operators) also represent a central object in finite volume QFT. Apart from the obvious relevance to lattice QFT they are also important in $1 + 1$ dimensional models, where they can be used to construct a systematic low-temperature expansion of correlation functions at finite temperature [9]. The connection to infinite volume form factors is given by a simple (though non-trivial) proportionality factor [10, 11, 12] which is exact to all orders in the inverse of the volume. There are however finite size corrections that decay exponentially with the volume and they play a crucial role whenever the numerical simulation is limited to small volumes. Moreover, they can

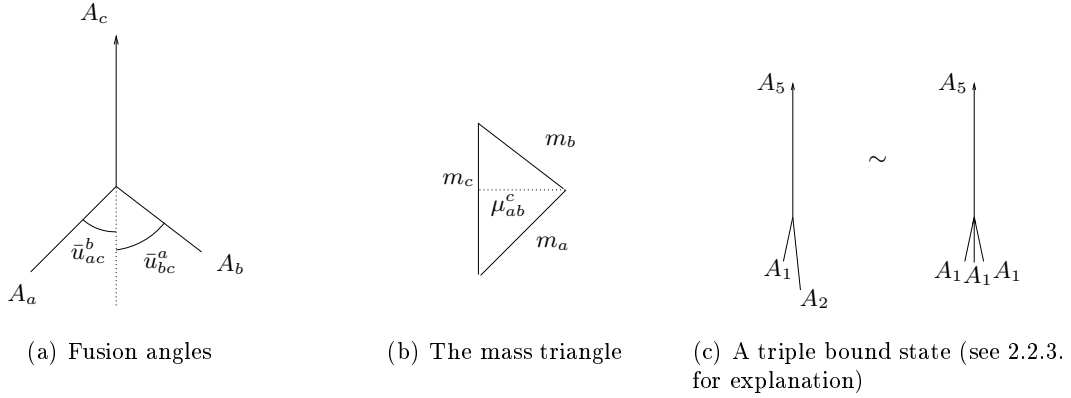


Figure 2.1: Pictorial representation of particle fusions.

produce huge deviations even in relatively large volumes provided that the exponent is small. This work was partly motivated by such an example which can be found in [12] (section 4.1.2).

In this work we present a method to obtain the leading μ -term associated to arbitrary multi-particle energy levels and finite volume form factors in 1 + 1 dimensional integrable models. Our approach is based on the idea that the μ -term is associated to the „inner structure“ of the particles, ie. their composition under the bootstrap program. It is supposed that the leading μ -term is caused by a symmetric particle fusion $A_a A_a \rightarrow A_c$. The results can also be applied in nonintegrable models for states below the first inelastic threshold.

The outline of the paper is as follows.

We begin our analysis in sec. 2 by giving a new interpretation of Lüscher’s μ -term and extending it to describe moving particles. The scaling Ising model serves as a testing ground for our calculations: the analytic predictions are compared to numerical data obtained by the Truncated Conformal Space Approach (TCSA) developed by Yurov and Zamolodchikov [13]. The extension of our results to arbitrary multi-particle scattering states is presented in section 3.

Section 4 deals with the μ -term of finite volume form factors and section 5 is devoted to the conclusions.

2 One-particle states

2.1 Bound-states in finite volume

Let us consider an integrable QFT with diagonal scattering. The spectrum consists of particles A_i , $i = 1, \dots, N$, with masses m_i which are assumed to be strictly non-degenerate. Asymptotic states are denoted by

$$|\theta_1, \theta_2, \dots, \theta_n\rangle_{i_1 i_2 \dots i_n},$$

where the indices $i_1 \dots i_n$ denote the particle species. Multi-particle scattering processes are described by the products of two-particle phase shifts $S_{ij}(\theta_{ij})$ where θ_{ij} is the relative rapidity of the incoming particles A_i and A_j .

The explicit formulas for the leading finite size mass corrections in a periodic box of volume L read [6]

$$\Delta m_a^{(\mu)} = - \sum'_{b,c} \theta(m_a^2 - |m_b^2 - m_c^2|) \mu_{ab}^c (\Gamma_{ab}^c)^2 e^{-\mu_{ab}^c L} \quad (2.1)$$

$$\Delta m_a^{(F)} = - \sum'_b \mathcal{P} \int_{-\infty}^{\infty} \frac{d\theta}{2\pi} e^{-m_b L \cosh(\theta)} m_b \cosh(\theta) (S_{ab}(\theta + i\pi/2) - 1) \quad (2.2)$$

μ_{ab}^c is the altitude of the mass triangle with base m_c (see figure 2.1) and $(\Gamma_{ab}^c)^2$ is the residue of $S_{ab}(\theta)$ corresponding to the formation of the bound state.

Here we determine the leading μ -term associated to a moving one-particle state A_c . Based on the description of mass corrections it is expected that this contribution is associated to the fusion $A_a A_b \rightarrow A_c$ with the smallest μ_{ab}^c . We assume that $a = b$, ie. the fusion in question is a symmetric one. This happens to be true for the lightest particle in models with the "Φ³-property" and for other low lying states in most known models. At the end of this section we comment on the possible extension to nonsymmetric fusions.

The bootstrap principle for a symmetric fusion consists of the identification

$$|\theta\rangle_c \sim |\theta + i\bar{u}_{ac}^a, \theta - i\bar{u}_{ac}^a\rangle_{aa} \quad (2.3)$$

resulting in

$$m_c = 2m_a \cos(\bar{u}_{ac}^a) \quad (\mu_{aa}^c)^2 = m_a^2 - \frac{m_c^2}{4}$$

Smallness of μ_{aa}^c means that m_c is close to $2m_a$, in other words the binding energy is small.

For a moment let us lay aside the framework of QFT and consider quantum mechanics with an attractive potential. Bound states are described by wave functions

$$\Psi(x_1, x_2) = e^{iP(x_1+x_2)}\psi(x_1 - x_2)$$

where P is the total momentum and $\psi(x)$ is the appropriate solution of the Schrödinger equation in the relative coordinate. It is localized around $x = 0$ and shows exponential decay at infinity. Except for the region $x_1 \approx x_2$, the wave function can be approximated with a product of plane waves with imaginary momenta $p_{1,2} = P \pm ik$. The interaction results in the quantization of the allowed values of k .

The theory in finite volume is described along the same lines. There are however two differences:

- The total momentum gets quantized.
- $\psi(x)$ (and therefore k) obtains finite volume corrections.

This picture also applies to relativistic integrable theories. We consider A_c as a simple quantum mechanical bound state of two elementary particles and use the infinite volume scattering data to describe the interaction between the constituents. To develop these ideas, let us consider the spectrum of the theory defined on a circle with circumference L . We state the identification

$$|A_c(\theta)\rangle_L \sim |A_a(\theta_1)A_a(\theta_2)\rangle_L \quad (2.4)$$

where the $\theta_{1,2}$ are complex to describe a bound-state; this idea also appeared in [14, 15]. Relation (2.4) can be regarded as the finite volume realization of (2.3). The total energy and momentum of the bound state have to be purely real, constraining the rapidities to take the form

$$\theta_1 = \theta + iu, \quad \theta_2 = \theta - iu \quad (2.5)$$

where the dependence on L is suppressed. Energy and momentum are calculated as

$$E = 2m_a \cos(u) \cosh(\theta) \quad p = 2m_a \cos(u) \sinh(\theta) \quad (2.6)$$

The momenta of two-particle states in finite volume are quantized by a relation involving the scattering phase shift [1]. This procedure can be extended in $1 + 1$ dimensional integrable models to arbitrary multi-particle scattering states. The quantization condition for an n -particle state is given by the Bethe-Yang equations

$$e^{ip_j L} \prod_{\substack{k=1 \\ k \neq j}}^n S_{i_j i_k}(\theta_j - \theta_k) = 1, \quad j = 1 \dots n$$

To quantize the bound state in finite volume, an appropriate analytic continuation of the above equations with $n = 2$ can be applied. This procedure is justified by the same reasoning that leads to original Bethe-Yang equations: one assumes plane waves (with imaginary momenta) except for

the localized interaction, which is described by the S-matrix of the infinite volume theory. Inserting (2.5) and separating the real and imaginary parts

$$e^{im_a \cos(u) \sinh(\theta)L} e^{-m_a \sin(u) \cosh(\theta)L} S_{aa}(2iu) = 1 \quad (2.7)$$

$$e^{im_a \cos(u) \sinh(\theta)L} e^{m_a \sin(u) \cosh(\theta)L} S_{aa}(-2iu) = 1 \quad (2.8)$$

Multiplying the two equations and making use of $S(2iu) = S(-2iu)^{-1}$ one arrives at

$$e^{2im_a \cos(u) \sinh(\theta)L} = 1 \quad \text{or} \quad 2m_a \cos(u) \sinh(\theta) = \frac{2\pi I}{L} \quad (2.9)$$

which is the quantization condition for the total momentum. I is to be identified with the momentum quantum number of A_c . The quantization condition for u is found by eliminating θ from (2.7):

$$e^{-m_a L \sin(u) \sqrt{1 + \left(\frac{\pi I}{m_a L \cos(u)}\right)^2}} S_{aa}(2iu) = (-1)^I \quad (2.10)$$

The exponential factor forces u to be close to the pole of the S-matrix associated to the formation of the bound-state. For the case at hand it reads

$$S_{aa}(\theta \sim iu_{aa}^c) \sim \frac{i(\Gamma_{aa}^c)^2}{\theta - iu_{aa}^c} \quad (2.11)$$

with $u_{aa}^c = 2\bar{u}_{ac}^a$. Note the appearance of $(-1)^I$ on the rhs. of (2.10), which is a natural consequence of the quantization of the total momentum. This sign determines the direction from which the pole is approached.

The exact solution of (2.10) can be developed into a power series in $e^{-\mu_{aa}^c L}$, where the first term is found by replacing u with \bar{u}_{ac}^a in the exponent:

$$u - \bar{u}_{ac}^a = (-1)^I \frac{1}{2} (\Gamma_{aa}^c)^2 e^{-\mu_{aa}^c L} \sqrt{1 + \left(\frac{2\pi I}{m_c L}\right)^2} + O(e^{-2\mu_{aa}^c L}) \quad (2.12)$$

First order corrections to the energy are readily evaluated to give

$$E = E_0 - (-1)^I (\Gamma_{aa}^c)^2 \frac{\mu_{aa}^c m_c}{E_0} e^{-\frac{\mu_{aa}^c E_0}{m_c} L} + O(e^{-2\mu_{aa}^c L}) \quad (2.13)$$

where E_0 is the ordinary one-particle energy

$$E_0 = \sqrt{m_c^2 + \left(\frac{2\pi I}{L}\right)^2}$$

In the case of zero momentum the former result simplifies to the leading term in (2.1). For large volumes we recover

$$u \rightarrow \bar{u}_{ac}^a \quad \theta \rightarrow \text{arsh} \frac{2\pi I}{m_c L}$$

Having established the quantization procedure we now turn to the question of momentum quantum numbers inside the bound state. For the phase shift let us adopt the convention introduced in [12]

$$S_{ab}(\theta) = S_{ab}(0) e^{i\delta_{ab}(\theta)}$$

where $\delta_{ab}(\theta)$ is defined to be continuous on the real line and is antisymmetric by unitarity and real analyticity. $\delta_{ab}(\theta)$ can be extended unambiguously to the imaginary axis by analytic continuation apart from the choice of the logarithmic branch. For a generic rapidity one has

$$\delta_{ab}(\theta^*) = \delta_{ab}(\theta)^* \quad \delta_{ab}(-\theta) = -\delta_{ab}(\theta)$$

Note that $\delta_{ab}(iu)$ is purely imaginary.

With this choice of the phase shift the Bethe-Yang equations in their logarithmic form

$$\begin{aligned} l \sinh(\theta + iu) + \delta_{11}(2iu) &= 2\pi I_1 \\ l \sinh(\theta - iu) + \delta_{11}(-2iu) &= 2\pi I_2 \end{aligned}$$

imply $I_1 = I_2$. Quantization of the total momentum on the other hand requires $I_1 = I_2 = I/2$. Note that different conventions for δ_{ab} would result in a less transparent rule for dividing I among the two constituents. The only disadvantage of our choice is the appearance of the unphysical half-integer quantum numbers.

Let us denote a multi-particle state in finite volume as

$$|\{I_1, \dots, I_n\}\rangle_{i_1 i_2 \dots i_n, L}$$

where the quantum numbers I_i serve as an input to the Bethe-Yang equations. The bound-state quantization can be written in short-hand notation as

$$|\{I\}\rangle_{c,L} \sim |\{I/2, I/2\}\rangle_{aa,L}$$

The example of mass corrections suggests that in order to obtain the total μ -term it is necessary to include a sum in (2.13) over the different fusions leading to A_c . However, the case of nonsymmetric fusions requires special care. Here we outline the difficulties of the nonsymmetric bound state quantization.

A straightforward application of the Bethe-Yang equations to an $|A_a(\theta + i\bar{u}_{ac}^b)A_b(\theta - i\bar{u}_{bc}^a)\rangle_L$ bound state yields a nontrivial phase factor $e^{2I\pi\frac{m_a}{m_a+m_b}}$ instead of $(-1)^I$ in (2.10). This in turn implies that the rapidity difference of the constituents can not be purely imaginary. The real parts of the rapidities thus get different finite size corrections and the total energy of the bound state becomes complex. A possible solution would be to take twice the real part of the energy correction, corresponding to the sum of the contributions coming from the $A_a A_b \rightarrow A_c$ and $A_b A_a \rightarrow A_c$ fusions. This is however only a guess and a more systematic treatment is needed. In fact, the infinite volume bootstrap principle suggests that the states

$$|A_a(\theta - i\bar{u}_{ac}^b)A_b(\theta + i\bar{u}_{bc}^a)\rangle_L \quad \text{and} \quad |A_a(\theta + i\bar{u}_{ac}^b)A_b(\theta - i\bar{u}_{bc}^a)\rangle_L$$

should be handled on an equal footing. A possible way to accomplish this would be to develop a multi-channel Bethe-Yang quantization scheme. However, this is beyond the scope of the present work.

As a conclusion of this section (2.12) is compared to the lowest order results of the TBA approach. The general discussion of excited states TBA equations in diagonal scattering theories is not available. For simplicity we restrict ourselves to the Lee-Yang model which was considered in the original paper [16]. In this nonunitary model there is only one particle and the scattering is described by

$$S(\theta) = \frac{\sinh(\theta) + i \sin(\pi/3)}{\sinh(\theta) - i \sin(\pi/3)}$$

The exact TBA equations for moving one-particle states read

$$E = -im(\sinh \theta_0 - \sinh \bar{\theta}_0) - \int_{-\infty}^{\infty} \frac{d\theta}{2\pi} m \cosh(\theta) L(\theta) \quad (2.14)$$

$$\varepsilon(\theta) = mR \cosh \theta + \log \frac{S(\theta - \theta_0)}{S(\theta - \bar{\theta}_0)} - (\varphi \star L)(\theta) \quad (2.15)$$

where

$$L(\theta) = \log(1 + e^{-\varepsilon(\theta)}) \quad \text{and} \quad (f \star g)(\theta) = \int_{-\infty}^{\infty} \frac{d\theta'}{2\pi} f(\theta - \theta')g(\theta')$$

Here the volume is denoted by R to avoid confusion with $L(\theta)$. The complex rapidity θ_0 satisfies the consistency equation

$$\varepsilon(\theta_0) = mR \cosh \theta_0 + i\pi - \log(S(2i\text{Im}\theta_0)) - (\varphi \star L)(\theta) = i(2n + 1)\pi \quad (2.16)$$

The convolution term in (2.16) can be neglected and one obtains $\text{Im}\theta_0 = \pi/6 + \delta$ where δ is exponentially small. To zeroth order one also has

$$mR \cosh(\text{Re}\theta_0) = (4n + (1 - \text{sign}\delta))\pi$$

which is the ordinary one-particle quantization condition with $I = 2n + \frac{1}{2}(1 - \text{sign}\delta)$. Neglecting the contribution of the integral in (2.14) and substituting $\theta_0 = \theta + iu$ one has $E = 2m \sin(u) \cosh(\theta)$. This is exactly the energy of an AA bound state with the imaginary rapidities $\theta \pm iu$. Separating the real and imaginary parts of (2.16) and still neglecting the convolution term (which is responsible for the F-term) one obtains equations (2.10) and (2.9), thus proving the consistency of the two approaches.

It seems plausible that by exactly solving the bound state quantization condition (2.10) one obtains all higher order corrections that go as $e^{-n\mu_{aa}^c L}$ with $n \in \mathbb{N}$. In the next subsection we present numerical evidence to support this claim.

2.2 Numerical analysis

We investigate the famous E_8 scattering theory [17], which is the relativistic integrable field theory associated to the scaling limit of the Ising model in the presence of a magnetic field. The infinite volume spectrum of the model consists of 8 particles. The first three particles lie below the two-particle threshold and they all show up as $A_1 A_1$ bound states. These fusions are responsible for the leading μ -term. The corresponding parameters (in units of m_1) are listed in the table below. The exponent of the next-to-leading correction (the error exponent) is denoted by μ' .

a	m_a	μ_{11}^a	$(\Gamma_{11}^a)^2$	μ'	
1	1	0.86603	205.14	1	(m_1)
2	1.6180	0.58779	120.80	0.95106	(μ_{12}^2)
3	1.9890	0.10453	1.0819	0.20906	$(2\mu_{11}^3)$

In [6] Klassen and Melzer performed the numerical analysis of mass corrections. The analytic predictions were compared to TCSA data and to transfer matrix results. They observed the expected behaviour of mass corrections of A_1 and A_2 ; in the former case they were also able to verify the F-term. On the other hand, the precision of their TCSA data was not sufficient to reach volumes where the μ -term for A_3 could have been tested. This limitation is a natural consequence of the unusually small exponent μ_{11}^3 : the next-to-leading contribution is of order $e^{-2\mu_{11}^3 L}$, still very slowly decaying.

Here we employ the TFCSA (Truncated Fermionic Conformal Space Approach, see [18]) routines that were successfully used in [9, 12]. Calculations are performed for $I = 0, 1, 2, 3$ at different values of the volume. One-particle states of A_1 , A_2 and A_3 are easily identified: they are the lowest lying levels in the spectrum, except for $I = 0$ where the lowest state is the vacuum. We use the dimensionless quantities $l = m_1 L$ and $e = E/m_1$.

The results are extrapolated from $e_{cut} = 20..30$ to $e_{cut} = \infty$ using the procedure developed in [19]. Our experience shows that this extrapolation technique reduces the numerical errors by an order of magnitude. However, our attempts to develop an adequate method to estimate these errors have failed. Several examples were encountered where the actual numerical deviation was either underestimated or overestimated, no matter which estimate was used. We therefore resign from quantitatively monitoring the TCSA errors and constrain ourselves to a range of the volume parameter where it is safe to neglect truncation effects.

2.2.1 A_3

We begin our analysis with the most interesting case of A_3 . At each value of l and I the following procedure is performed.

- The energy correction is calculated according to (2.13)
- The quantization condition (2.10) is solved for u and the energy correction is calculated by

$$\Delta e = 2 \cosh(\theta) \cos(u) - e_0$$

where θ is determined by the total momentum quantization (2.9) and e_0 is the ordinary one-particle energy.

- The exact correction is calculated numerically by $\Delta e = e^{TCSA} - e_0$.

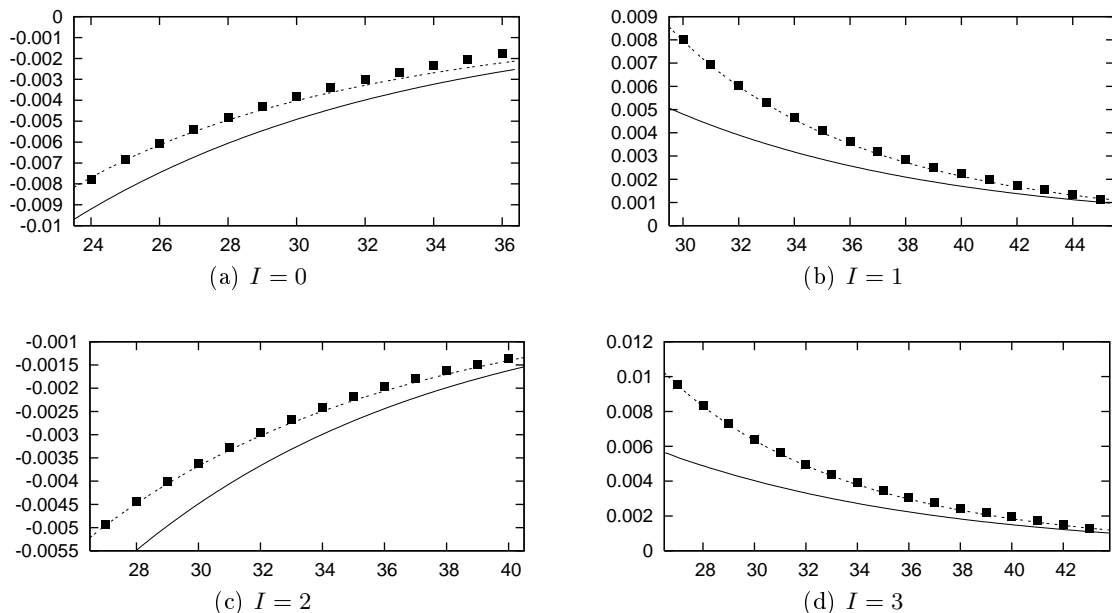


Figure 2.2: Finite size corrections to A_3 one-particle levels (in sectors $I = 0 \dots 3$) as a function of the volume. The TCSA data are plotted against theoretical predictions of the single μ -term associated to the $A_1 A_1 \rightarrow A_3$ fusion (solid curve) and the exact solution of the bound-state quantization (dotted curve).

The choice for the range of the volumes is limited in two ways. On one hand, l has to be sufficiently large in order to reduce the contribution of the F terms and other higher order finite size corrections. On the other hand, numerical errors grow with the volume and eventually become comparable with the finite size corrections, resulting in an upper bound on l . The window $l = 30..40$ is suitable for our purposes.

The results are shown in figure 2.2. It is clear that the μ -term yields the correct prediction in the $L \rightarrow \infty$ limit. However, higher order terms cause a significant deviation for $l < 40$, which is in turn accurately described by the bound state prediction. The sign of the correction depends on the parity of I as predicted by (2.13).

Based on the success of this first numerical test we also explored the region $l < 30$. Inspecting the behaviour of u as a function of l reveals an interesting phenomenon. It is obvious from (2.12) that $u(l)$ is monotonously increasing if I is odd, with the infinite volume limit fixed to \bar{u}_{ac}^a . However, the complex conjugate pair $\theta_{1,2}$ approaches the real axis as l is decreased and they collide at a critical volume $l = l_c$. For $l < l_c$ they separate again but stay on the real line, providing a unique solution with two distinct purely real rapidities. The same behaviour was also observed in [14, 15].

The interpretation of this phenomenon is evident: if the volume is comparable to the characteristic size of the bound-state, there is enough energy in the system for the constituents to become unbound. Therefore the A_3 one-particle level becomes an $A_1 A_1$ scattering state for $l < l_c$. We call this phenomenon the “dissociation of the bound state”. The same result was obtained also in the boundary sine-Gordon model by a semiclassical analysis [20].

The value of l_c can be found by exploiting the fact that the Jacobian of the Bethe-Yang equations (viewed as a mapping from (θ_1, θ_2) to (I_1, I_2)) vanishes at the critical point. A straightforward calculation yields

$$l_c = \sqrt{4\varphi_{11}(0)^2 - I^2\pi^2}$$

where $\varphi_{11}(\theta) = \delta'_{11}(\theta)$. The numerical values for the case at hand are

$$l_c = 27.887 \quad (I = 1) \quad \text{and} \quad l_c = 26.434 \quad (I = 3)$$

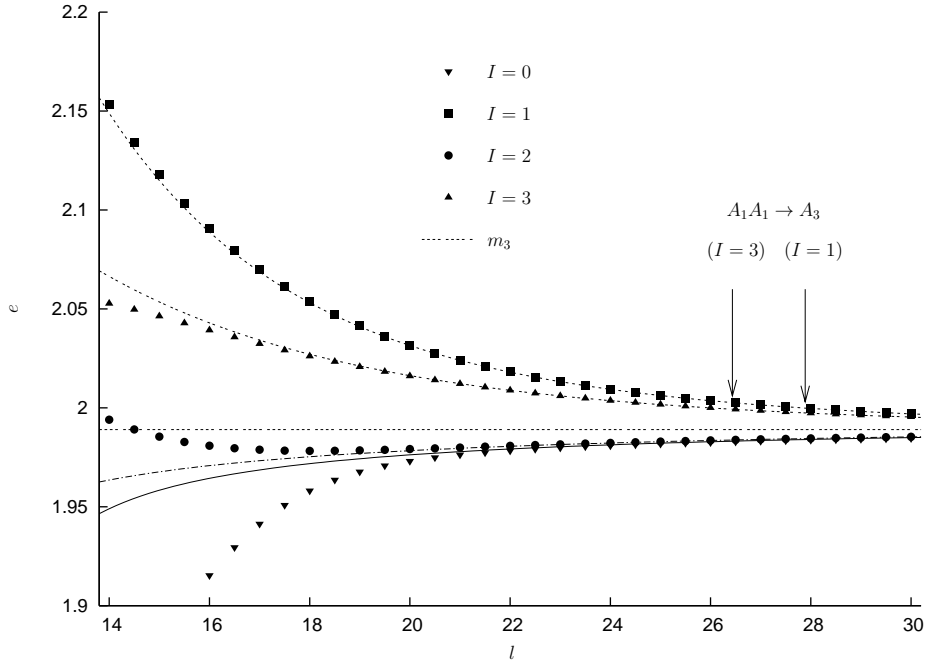


Figure 2.3: A_3 one-particle levels in sectors $I = 0 \dots 3$ as a function of the volume. Dots represent TCSA data, while the lines show the corresponding prediction of the A_1A_1 bound state quantization. In sectors $I = 1$ and $I = 3$ the bound state dissociates at l_c and for $l < l_c$ a conventional A_1A_1 scattering state replaces A_3 in the spectrum. The values of l_c are shown by the two arrows.

We are now in the position to complete the numerical analysis. The Bethe-equations are solved at each value of l , providing two distinct real rapidities for $l < l_c$ (with I being odd), and a complex conjugate pair otherwise. The energy is calculated in either case as

$$e = \cosh(\theta_1) + \cosh(\theta_2)$$

which is compared to TCSA data. The results are exhibited in figure 2.3.

The agreement for the upper two curves ($I = 1$ and $I = 3$) is not as surprising as it may seem because what one sees here are conventional A_1A_1 scattering states. The Bethe-Yang equation determining their energy is exact up to $O(e^{-\mu' L})$ where $\mu' = \mu_{11}^1$ is the smallest exponent that occurs in the sequence of finite volume corrections of A_1 . On the other hand, the energy levels are analytic functions of L , which leads to the conclusion that the prediction of (2.10) is correct up to $O(e^{-\mu_{11}^1 L})$ even for $L > L_c$. Comparing the numerical values one finds $\mu_{11}^1 > 8\mu_{11}^3$. We conclude that the bound state picture indeed accounts for finite volume corrections up to the first few orders in $e^{-\mu_{aa}^c L}$ (the first 8 orders in the case at hand).

2.2.2 A_1 and A_2

Particles A_1 and A_2 also appear as A_1A_1 bound states. However, there is no point in applying the complete bound state quantization to them, because the error terms dominate over the higher order contributions from (2.10): the exponents of the subleading finite size corrections m_1 and μ_{12}^2 are smaller than $2\mu_{11}^1$ and $2\mu_{11}^2$. Nevertheless, the leading μ -term can be verified by choosing suitable windows in l .

In figures A.1 and A.2 $\log(|\Delta e|)$ is plotted against the prediction of (2.13) for $l = 6..16$ and $l = 6..22$. (the sign of Δe was found to be in accordance with (2.13) for both A_1 and A_2)

In the case of A_1 perfect agreement is observed for $l = 10..18$ in the sectors $I = 0$ and $I = 1$.

For $I = 2$ and $I = 3$ the energy corrections become too small and therefore inaccessible to TCSA (note that the prediction for $I = 3$ is of order 10^{-6}).

In the case of A_2 precise agreement is found for $l = 14.22$ in all four sectors.

2.2.3 A_5

Here we present an interesting calculation that determines the leading mass corrections of A_5 . The standard formulas are inapplicable in this case, because m_5 lies above the two-particle threshold. However, it is instructive to consider the composition of A_5 under the bootstrap principle and to evaluate the μ -term prediction.

There are two relevant fusions

$$\begin{aligned} A_1 A_3 &\rightarrow A_5 & \text{with } \mu_{13}^5 &= 0.2079 \\ A_2 A_2 &\rightarrow A_5 & \text{with } \mu_{22}^5 &= 0.6581 \end{aligned}$$

Numerical evaluation of (2.1) shows that the contribution of the second fusion is negligible for $l > 30$. The first fusion on the other hand yields a significant discrepancy when compared to TCSA data. This failure is connected to the two-particle threshold and it can be explained in terms of the bound state quantization. Experience with A_3 suggests that one should first take into account the energy corrections of A_3 and consider the $A_1 A_3 \rightarrow A_5$ fusion afterwards. A_3 can be split into $A_1 A_1$ leading to the "triple bound state" $A_1 A_1 A_1 \rightarrow A_5$. In infinite volume one has (see also fig. 2.1 c.)

$$|\theta\rangle_5 \sim |\theta - 2i\bar{u}_{11}^3, \theta, \theta + 2i\bar{u}_{11}^3\rangle_{111}$$

The finite volume realization of this identification is most easily carried out in the $I = 0$ sector with

$$|\{0\}\rangle_{5,L} \sim |\{0, 0, 0\}\rangle_{111,L}$$

Setting up the three-particle Bethe-Yang equations with rapidities $(iu, 0, -iu)$:

$$\begin{aligned} e^{-m_1 \sin(u)L} S_{11}(iu) S_{11}(2iu) &= 1 \\ S_{11}(iu) S_{11}(-iu) &= 1 \\ e^{m_1 \sin(u)L} S_{11}(-iu) S_{11}(-2iu) &= 1 \end{aligned}$$

The second equation is automatically satisfied due to unitarity and real analyticity, whereas the first and the third are equivalent and they serve as a quantization condition for u . The finite volume mass of A_5 is given in terms of the solution by

$$m_5(l) = 2 \cos(u) + 1 \tag{2.17}$$

In the large L limit the infinite volume mass is reproduced by $u \rightarrow 2\bar{u}_{11}^3$. Figure 2.4 demonstrates the agreement between TCSA and the prediction of (2.17).

The possibility of solving the quantization of the triple bound state in a moving frame looks very appealing. In the general case the rapidities are expected to take the form $(\theta_1 + iu, \theta_2, \theta_1 - iu)$ where θ_1 and θ_2 do not necessarily coincide. However, the numerical precision of our TCSA data was not sufficient to check our predictions.

3 Multi-particle states

3.1 Bethe-Yang quantization in the bound state picture

Multi-particle states in finite volume are denoted by

$$|\{I_1, \dots, I_n\}\rangle_{i_1 i_2 \dots i_n, L}$$

where the quantum numbers I_j serve as an input to the Bethe-Yang equations

$$Q_j(\theta_1, \dots, \theta_n) = m_{i_j} \sinh(\theta_j)L + \sum_{k \neq j} \delta_{i_j i_k} (\theta_j - \theta_k) = 2\pi I_j \quad j = 1 \dots n \tag{3.1}$$

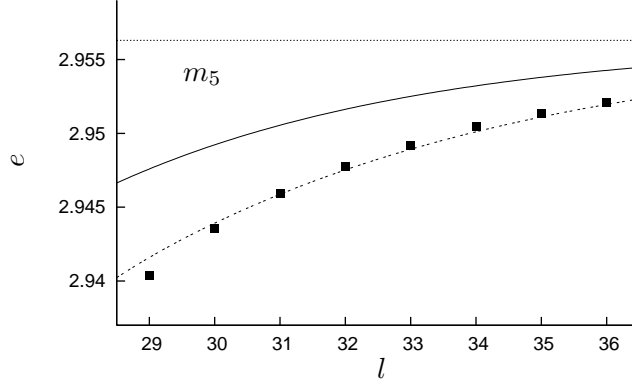


Figure 2.4: Finite size mass of A_5 as a function of the volume. The squares represent the TCSA data which is compared to the leading μ -term (solid curve) and the solution of the quantization condition for the “triple bound state“ $A_1 A_1 A_1$ (dotted curve). The straight line shows the infinite volume mass.

The energy is calculated as

$$E = \sum_{j=1}^n m_{i_j} \cosh(\bar{\theta}_j) + \dots \quad (3.2)$$

where $(\bar{\theta}, \bar{\theta}_1, \dots, \bar{\theta}_n)$ is the solution of (3.1). The dots indicate exponentially decaying finite size corrections.

Let us consider a scattering state $|\{I, I_1, \dots, I_n\}\rangle_{cb_1 \dots b_n, L}$ composed of $n+1$ particles, the first one being A_c . We determine the leading part of the μ -term by considering A_c as an $A_a A_a$ bound state *inside the multi-particle state*. Therefore we write

$$|\{I, I_1, \dots, I_n\}\rangle_{cb_1 \dots b_n, L} \sim |\{I/2, I/2, I_1, \dots, I_n\}\rangle_{aab_1 \dots b_n, L} \quad (3.3)$$

The energy is then determined by analytic continuation of the $n+2$ particle Bethe-Yang equations. They read

$$e^{-m_a \sin(u) \cosh(\theta)L} e^{im_a \cos(u) \sinh(\theta)L} S_{aa}(2iu) \prod_{j=1}^n S_{ab_j}(\theta + iu - \theta_j) = 1 \quad (3.4)$$

$$e^{m_a \sin(u) \cosh(\theta)L} e^{im_a \cos(u) \sinh(\theta)L} S_{aa}(-2iu) \prod_{j=1}^n S_{ab_j}(\theta - iu - \theta_j) = 1 \quad (3.5)$$

$$e^{im_{b_j} \sinh(\theta_j)L} S_{ab_j}(\theta_j - \theta - iu) S_{ab_j}(\theta_j - \theta + iu) \prod_{\substack{k=1 \\ k \neq j}}^n S_{b_j b_k}(\theta_j - \theta_k) = 1 \quad (3.6)$$

The ordinary $n+1$ particle Bethe-equations are reproduced in the $L \rightarrow \infty$ limit by multiplying (3.4) and (3.5) and making use of the bootstrap equation

$$S_{cb_j}(\theta) = S_{ab_j}(\theta + i\bar{u}_{ac}^a) S_{ab_j}(\theta - i\bar{u}_{ac}^a)$$

We now proceed similar to the previous section and derive a formula for the leading correction. The shift in the imaginary part of the rapidity can be calculated by making use of (3.4) and (2.11) as

$$\Delta u = u - \bar{u}_{ac}^a = \frac{(\Gamma_{aa}^c)^2}{2} e^{-\mu \cosh(\bar{\theta})L} e^{im_c \sinh(\bar{\theta})L/2} \prod_{j=1}^n S_{ab_j}(\bar{\theta} + i\bar{u}_{ac}^a - \bar{\theta}_j) \quad (3.7)$$

Multiplying (3.4) and (3.5)

$$e^{i2m_a \cos(u) \sinh(\theta)L} \prod_{j=1}^n S_{ab_j}(\theta - iu - \theta_j) S_{ab_j}(\theta + iu - \theta_j) = 1 \quad (3.8)$$

$$e^{im_{b_j} \sinh(\theta_j)L} S_{ab_j}(\theta_j - \theta - iu) S_{ab_j}(\theta_j - \theta + iu) \prod_{\substack{k=1 \\ k \neq j}}^n S_{b_j b_k}(\theta_j - \theta_k) = 1 \quad (3.9)$$

Let us define

$$S_{ab_j}(\theta - iu - \theta_j) S_{ab_j}(\theta + iu - \theta_j) \approx S_{cb_j}(\theta - \theta_j) e^{i\Delta u \bar{\varphi}_{cb_j}(\theta - \theta_j)}$$

where

$$\bar{\varphi}_{cb_j}(\theta) = i\varphi_{cb_j}(\theta + i\bar{u}_{ac}^a) - i\varphi_{cb_j}(\theta - i\bar{u}_{ac}^a) \quad \text{with} \quad \varphi_{ab}(\theta) = \delta'_{ab}(\theta)$$

Using $2m_a \cos(u) \approx m_c - 2\mu_{aa}^c \Delta u$ the logarythm of (3.8) and (3.9) can be written as

$$\begin{aligned} Q_0(\theta, \theta_1, \dots, \theta_n) &= \left(2\mu_{aa}^c \sinh(\theta)L - \sum_{j=1}^n \bar{\varphi}_{cb_j}(\theta - \theta_j) \right) \Delta u \\ Q_j(\theta, \theta_1, \dots, \theta_n) &= \bar{\varphi}_{cb_j}(\theta - \theta_j) \Delta u \end{aligned}$$

The lhs. can be expanded around the $n + 1$ particle solution $(\bar{\theta}, \bar{\theta}_1, \dots, \bar{\theta}_n)$ to arrive at

$$\begin{pmatrix} \theta - \bar{\theta} \\ \theta_1 - \bar{\theta}_1 \\ \vdots \\ \theta_n - \bar{\theta}_n \end{pmatrix} = \left(\mathcal{J}^{(n+1)} \right)^{-1} \begin{pmatrix} 2\mu_{aa}^c \sinh(\bar{\theta})L - \sum_{j=1}^n \bar{\varphi}_{cb_j}(\bar{\theta} - \bar{\theta}_j) \\ \bar{\varphi}_{cb_1}(\bar{\theta} - \bar{\theta}_1) \\ \vdots \\ \bar{\varphi}_{cb_n}(\bar{\theta} - \bar{\theta}_n) \end{pmatrix} \Delta u \quad (3.10)$$

where

$$\mathcal{J}_{kl}^{(n+1)} = \frac{\partial Q_k}{\partial \theta_l}$$

The final result for the energy correction reads

$$\Delta E = -2\mu_{aa}^c \cosh(\bar{\theta}) \Delta u + \begin{pmatrix} m_c \sinh(\bar{\theta}) \\ m_{b_1} \sinh(\bar{\theta}_1) \\ \vdots \\ m_{b_n} \sinh(\bar{\theta}_n) \end{pmatrix} \left(\mathcal{J}^{(n+1)} \right)^{-1} \begin{pmatrix} 2\mu_{aa}^c \sinh(\bar{\theta})L - \sum_{j=1}^n \bar{\varphi}_{cb_j}(\bar{\theta} - \bar{\theta}_j) \\ \bar{\varphi}_{cb_1}(\bar{\theta} - \bar{\theta}_1) \\ \vdots \\ \bar{\varphi}_{cb_n}(\bar{\theta} - \bar{\theta}_n) \end{pmatrix} \Delta u \quad (3.11)$$

with Δu given by (3.7).

Based on the previous section it is expected that there is a similar contribution for every fusion leading to each one of the constituents of the multi-particle state.

3.2 Multi-particle states – Numerical analysis

We first consider finite size corrections to $A_1 A_3$ states. They are not the lowest lying two-particle states in the spectrum, but they possess the largest μ -term which is connected to the $A_1 A_1 \rightarrow A_3$ fusion. Given a particular state $|\{I_1, I_3\}\rangle_{13,L}$ the following procedure is performed at each value of the volume:

- The two-particle Bethe-Yang equation for $|\{I_1, I_3\}\rangle_{13,L}$ is solved and the μ -term is calculated according to (3.11).
- The exact three-particle Bethe-Yang equation is solved for $|\{I_1, I_3/2, I_3/2\}\rangle_{111,L}$

The results for different $A_1 A_3$ levels are shown in figure A.3. The situation is similar to the case of the A_3 one-particle levels: the bound state quantization yields a remarkably accurate prediction, whereas the single μ -term prediction only becomes correct in the $L \rightarrow \infty$ limit.

In table A.1 we present a numerical example for the dissociation of the bound state inside the two-particle state. In this case an $A_1 A_3$ state turns into a conventional $A_1 A_1 A_1$ three-particle state at $l_c \approx 30$.

Finite size corrections to $A_1 A_1$ and $A_1 A_2$ states are also investigated, the leading μ -term given by the fusions $A_1 A_1 \rightarrow A_1$ and $A_1 A_1 \rightarrow A_2$, respectively. In the former case we calculate separately the contribution associated to both A_1 particles and add them to get the total correction. Results are exhibited in figures A.4 and A.5 and formula (3.11) is verified in both cases.

4 Finite volume form factors

The connection between finite volume and infinite volume form factors was derived in [12] as

$$F^\mathcal{O}(\bar{\theta}'_m + i\pi, \dots, \bar{\theta}'_1 + i\pi, \bar{\theta}_1, \dots, \bar{\theta}_n)_{j_m \dots j_1 i_1 \dots i_n} = \frac{F^\mathcal{O}(\bar{\theta}'_m + i\pi, \dots, \bar{\theta}'_1 + i\pi, \bar{\theta}_1, \dots, \bar{\theta}_n)_{j_m \dots j_1 i_1 \dots i_n}}{\sqrt{\rho_{i_1 \dots i_n}(\bar{\theta}_1, \dots, \bar{\theta}_n) \rho_{j_1 \dots j_m}(\bar{\theta}'_1, \dots, \bar{\theta}'_m)}} + O(e^{-\mu' L}) \quad (4.1)$$

where the rapidities $\bar{\theta}$ are solutions of the corresponding Bethe-Yang equations and it is supposed that $\bar{\theta}_j \neq \bar{\theta}'_k$ whenever $i_j = i_k$. The extension of (4.1) to include disconnected terms can be found in [9]. The proportionality factor in (4.1) is given by the density of states

$$\rho_{i_1 \dots i_n}^{(n)}(\bar{\theta}_1, \dots, \bar{\theta}_n) = \det \mathcal{J}^{(n)} \quad , \quad \mathcal{J}_{kl}^{(n)} = \frac{\partial Q_k}{\partial \theta_l} \quad , \quad k, l = 1 \dots n$$

which can be used to identify formally the finite volume and infinite volume states as

$$|\{I_1, \dots, I_n\}\rangle_{i_1 i_2 \dots i_n, L} \sim \frac{1}{\sqrt{\rho_{i_1 \dots i_n}^{(n)}(\bar{\theta}_1, \dots, \bar{\theta}_n)}} |\bar{\theta}_1, \dots, \bar{\theta}_n\rangle_{i_1 \dots i_n}$$

Based on general arguments it was shown in [12] that $\mu' \geq \mu$ where μ is determined by the pole of the S-matrix closest to the physical line. A systematic finite volume perturbation theory (Lüscher's method applied to form factors) is not available. However, it is expected that the actual value of μ' depends on what diagrams contribute to the form factor in question. Apart from the insertion of the local operator they coincide with the diagrams determining the finite size corrections of the multi-particle state. Therefore μ' is associated to the bound state structure of the constituents of the multi-particle state. In this section it is shown that the leading correction term can be obtained by the bound state quantization.

4.1 Elementary one-particle form factors

(4.1) yields a simple prediction for the elementary one-particle form factor:

$$F_c^\mathcal{O}(I, L) \equiv \langle 0 | \mathcal{O}(0, 0) | \{I\} \rangle_{c, L} = \frac{F_c^\mathcal{O}}{\sqrt{EL}} + O(e^{-\mu' L}) \quad (4.2)$$

where E is the one-particle energy, and $F_c^\mathcal{O} = F_c^\mathcal{O}(\theta)$ is the infinite volume one-particle form factor, which is constant by Lorentz symmetry.

The μ -term associated to (4.2) is derived by employing the bound state quantization. We gain some intuition from the previous sections where it was found that the bound state $A_a A_a$ may dissociate at a critical volume L_c . For $L < L_c$ there is no one-particle level of type A_c in the given sector of the spectrum, however an $A_a A_a$ scattering state appears instead. Finite volume form factors of this state are calculated using (4.1) as

$$F_c^\mathcal{O}(I, L) = \frac{F^\mathcal{O}(\theta_1, \theta_2)_{aa}}{\sqrt{\rho_{aa}(\theta_1, \theta_2)}} \quad \text{for } L < L_c \quad (4.3)$$

The generalization to $L > L_c$ seems to be straightforward: one has to continue analytically (4.3) to the solutions of the Bethe-Yang equation with imaginary rapidities $\theta_{1,2} = \theta \pm iu$. However, note

that equations (4.2) and (4.3) are valid up to a phase factor. In order to continue analytically to imaginary rapidities we also need to fix this phase¹.

The two-particle form factor satisfies

$$F^\mathcal{O}(\theta_1, \theta_2)_{aa} = S_{aa}(\theta_1 - \theta_2) F^\mathcal{O}(\theta_2, \theta_1)_{aa}$$

The simplest choice for the phase is therefore

$$F^\mathcal{O}(\theta_1, \theta_2)_{aa} = \sqrt{S_{aa}(\theta_1 - \theta_2)} |F^\mathcal{O}(\theta_1, \theta_2)_{aa}| \quad (4.4)$$

This choice is dictated by CPT symmetry [21, 10, 11], and it is respected by all known solutions of the form factor bootstrap axioms. There is a sign ambiguity caused by the square root, but it can be fixed by demanding $(S_{aa}(0))^{1/2} = i$ and continuity. Using (4.4)

$$F_c^\mathcal{O}(I, L) = \frac{\sqrt{S_{aa}(\theta_2 - \theta_1)} F^\mathcal{O}(\theta_1, \theta_2)_{aa}}{\sqrt{\rho_{aa}(\theta_1, \theta_2)}}$$

and upon analytic continuation

$$F_c^\mathcal{O}(I, L) = \frac{\sqrt{S_{aa}(-2iu)} F^\mathcal{O}(\theta + iu, \theta - iu)_{aa}}{\sqrt{\rho_{aa}(\theta + iu, \theta - iu)}} \quad \text{for } L > L_c \quad (4.5)$$

It is easy to see that the result (4.2) is reproduced in the $L \rightarrow \infty$ limit. First observe that

$$F^\mathcal{O}(\theta + iu, \theta - iu)_{aa} \sim \frac{\Gamma_{aa}^c}{2(u - \bar{u}_{ac}^a)} F_c^\mathcal{O}(\theta)$$

The residue of ρ_{aa} is determined by $\varphi_{aa}(2iu)$ and it reads

$$\rho(\theta + iu, \theta - iu)_{aa} \sim 2m_a L \cos(u) \cosh(\theta) (-i) \frac{S'_{aa}(2iu)}{S_{aa}(2iu)} = m_c L \cosh(\theta) \frac{1}{2(u - \bar{u}_{ac}^a)}$$

The singularities in the numerator and denominator of (4.5) cancel and indeed

$$F_c^\mathcal{O}(I, L) \sim \frac{F_c^\mathcal{O}}{\sqrt{m_c L \cosh(\theta)}}$$

We emphasize that it is crucial to include the extra normalisation factor $\sqrt{S_{aa}(-2iu)}$ to obtain a meaningful result.

Expression (4.5) can be developed into a Taylor-series in $u - \bar{u}_{ac}^a$. The first order correction is evaluated in Appendix A and it reads

$$\begin{aligned} F_c^\mathcal{O}(I, L) &= \frac{F_c^\mathcal{O}}{\sqrt{E_c^0 L}} - \frac{2i\Gamma_{aa}^c (F_{aa}^\mathcal{O})'}{\sqrt{E_c^0 L}} (u - \bar{u}_{ac}^a) + \\ &+ \frac{F_c^\mathcal{O}}{\sqrt{E_c^0 L}} \left[\frac{2S_{aa}^{c,0}}{(\Gamma_{aa}^c)^2} + \frac{m_c \mu}{(E_c^0)^2} - \left(\frac{m_a^2}{m_c^2} E_c^0 - \frac{\mu^2}{E_c^0} \right) L \right] (u - \bar{u}_{ac}^a) + O(e^{-2\mu L}) \end{aligned} \quad (4.6)$$

where

$$\begin{aligned} (F_{aa}^\mathcal{O})' &= \lim_{\theta - \theta' = -2i\bar{u}_{ac}^a} \frac{d}{d\theta} F^\mathcal{O}(\theta, \theta')_{aa} \\ S_{aa}^{c,0} &= \lim_{u \rightarrow \bar{u}_{ac}^a} \left(S_{aa}(2iu) - \frac{(\Gamma_{aa}^c)^2}{2(u - \bar{u}_{ac}^a)} \right) \end{aligned}$$

E_c^0 is the ordinary one-particle energy and the rapidity shift $u - \bar{u}_{ac}^a$ is given by (2.12).

¹The phase of a (nondiagonal) infinite volume form factor is unphysical in the sense that it may be redefined by a complex rotation of the state vectors and physical quantities, e.g. correlation functions, do not depend on such redefinitions. However, the bootstrap program uniquely assigns a phase to each form factor.

4.2 One-particle form factors – Numerical analysis

Let us introduce the dimensionless form factors as

$$f_i(I, l) = \frac{\langle 0 | \varepsilon(0, 0) | \{I\} \rangle_{i, L}}{m_1}$$

The machinery of [12] is used to determine $f_i(I, l)$ for $i = 1, 2, 3$ and $I = 0, 1, 2, 3$. The numerical results are compared to the exact infinite volume form factors [22, 23].

We start our investigation with $f_3(I, l)$, for which relatively large exponential corrections were already reported in [12]. It is convenient to consider

$$\bar{f}_3(I, l) = (e_0 l)^{1/2} f_3(I, L) \quad \text{with} \quad \lim_{l \rightarrow \infty} \bar{f}_3(I, l) = F_3 \quad (4.7)$$

The numerical results are demonstrated in fig. 4.1. Note, that this is exactly the same figure as 4.6. (c) in [12], but this time the interpretation of the huge deviations from F_3 is also provided.

We also tried to verify the predictions for f_1 and f_2 . In the latter case reasonably good agreement was found with TCSA, the results are demonstrated in fig. A.6. In the case of f_1 we encountered the unpleasant situation that the F-term decays slower than the TCSA errors grow, thus making the observation of the μ -term impossible.

It is straightforward to generalize (4.5) to matrix elements between two different one-particle states. For $b \neq c$ one has for example

$${}_b \langle \{I_b\} | \varepsilon | \{I_c\} \rangle_{c, L} = \frac{F^\varepsilon(\theta_b + i\pi, \theta + iu, \theta - iu)_{baa}}{\sqrt{\rho_b(\theta_b) \rho_{aa}(\theta + iu, \theta - iu)}}$$

Numerical examples are presented in figures 4.2 (a)-(c) for $c = 3$ and $b = 1, 2$.

The most interesting case is the one shown in fig. 4.2 (d) where the matrix element between two different A_3 one-particle states are investigated. This can be done by considering both A_3 particles as the appropriate $A_1 A_1$ bound states and then calculating the finite volume form factor ${}_3 \langle \{I\} | \varepsilon | \{I'\} \rangle_{3, L}$ as

$${}_{11} \langle \{I/2, I/2\} | \varepsilon | \{I'/2, I'/2\} \rangle_{11, L} = \frac{F^\varepsilon(\theta + iu + i\pi, \theta - iu + i\pi, \theta' + iu', \theta' - iu')_{1111}}{\sqrt{\rho_{11}(\theta' + iu', \theta' - iu') \rho_{11}(\theta + iu, \theta - iu)}}$$

Once again we find complete agreement with the TCSA data.

4.3 Elementary multi-particle form factors

The generalization of (4.5) to multi-particle states is straightforward, the only task is to find the appropriate phase factor. Similar to the one-particle case one has

$$F^\mathcal{O}(\theta_1, \dots, \theta_m)_{b_1 \dots b_m} = \sqrt{\prod_{i < j} S_{b_i b_j}(\theta_i - \theta_j)} |F^\mathcal{O}(\theta_1, \dots, \theta_m)_{b_1 \dots b_m}|$$

A general n particle finite volume form factor with real rapidities can thus be written as

$$\sqrt{\frac{\prod_{i < j} S_{b_i b_j}(\theta_j - \theta_i)}{\rho^n(\theta_1, \dots, \theta_n)_{b_1 \dots b_n}}} F^\mathcal{O}(\theta_1, \dots, \theta_n)_{b_1 \dots b_n}$$

Substituting the solution of the Bethe-equation for the state $|\{I/2, I/2, I_1, \dots, I_n\}\rangle_{aab_1 \dots b_n, L}$ and making use of the real analyticity condition

$$|S_{ab_j}(\theta_j - \theta - iu) S_{ab_j}(\theta_j - \theta + iu)| = 1$$

one gets

$$\langle 0 | \mathcal{O} | \{I/2, I/2, I_1, \dots, I_n\} \rangle_{aab_1 \dots b_n, L} = \frac{\sqrt{S_{aa}(-2iu)} |F^\mathcal{O}(\theta + iu, \theta - iu, \theta_1, \dots, \theta_n)_{aab_1 \dots b_n}|}{\sqrt{\rho^{(n+2)}(\theta + iu, \theta - iu, \theta_1, \dots, \theta_n)_{aab_1 \dots b_n}}} \quad (4.8)$$

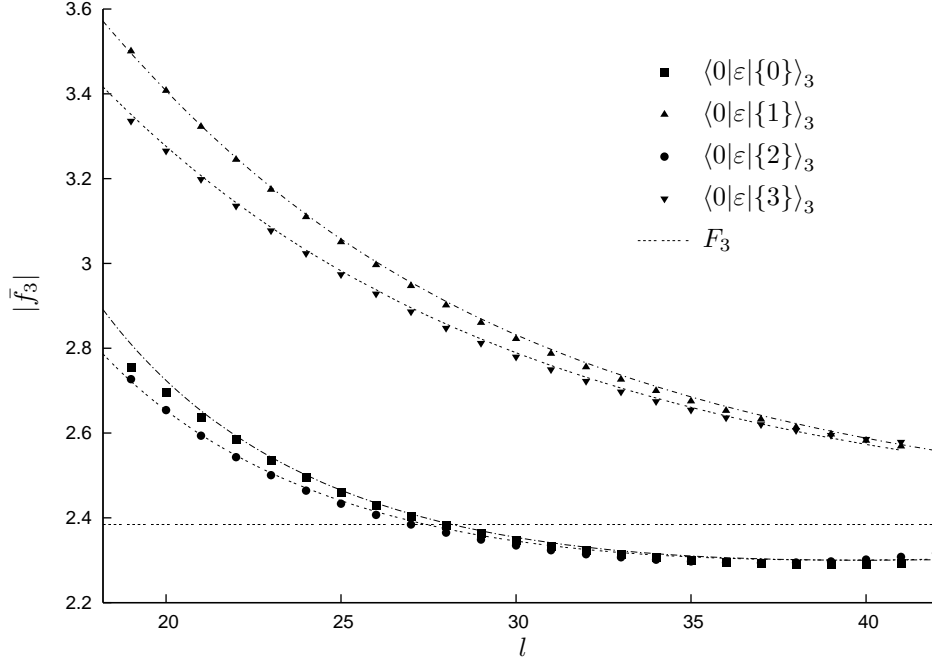


Figure 4.1: Elementary finite volume form factors of A_3 one-particle levels. Here the normalization (4.7) is applied to obtain a finite $l \rightarrow \infty$ limit, which is given by the infinite volume form factor $F_3 = \langle 0|\varepsilon|A_3(\theta)\rangle$. The TCSA data are plotted against the bound state prediction. The ordinary evaluation of \bar{f}_3 is simply the constant F_3 .

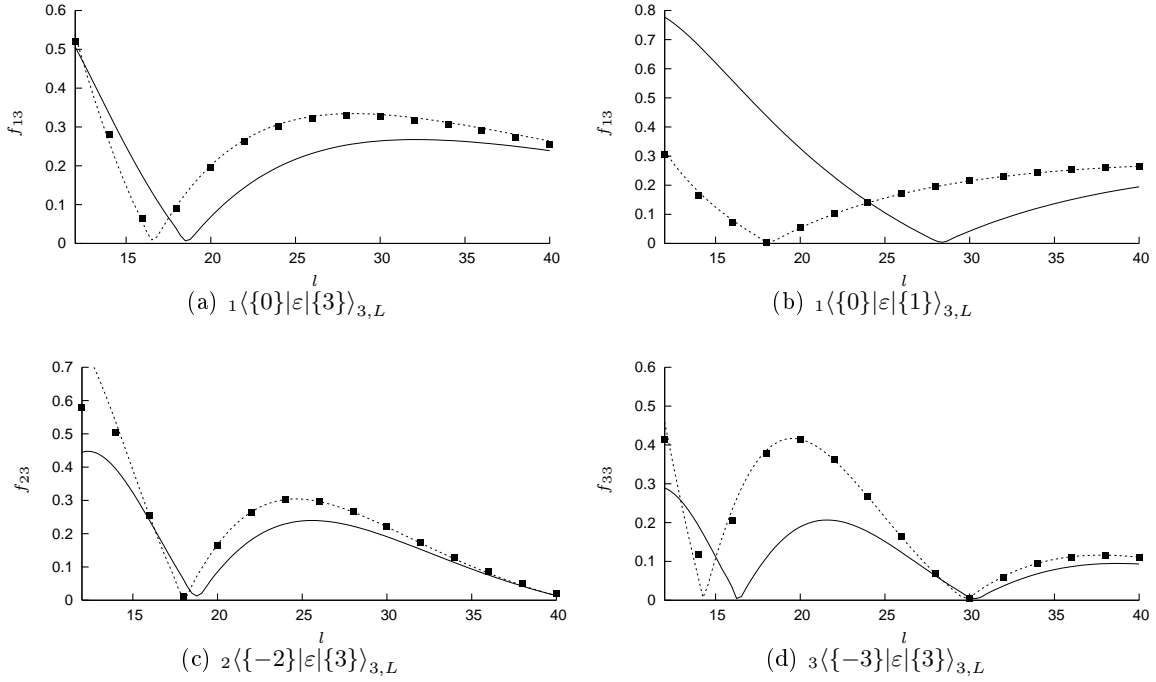


Figure 4.2: One-particle-one-particle form factors, dots correspond to TCSA data. The solid lines represent the ordinary evaluation of the finite volume form factors, while the dotted lines show the bound state prediction.

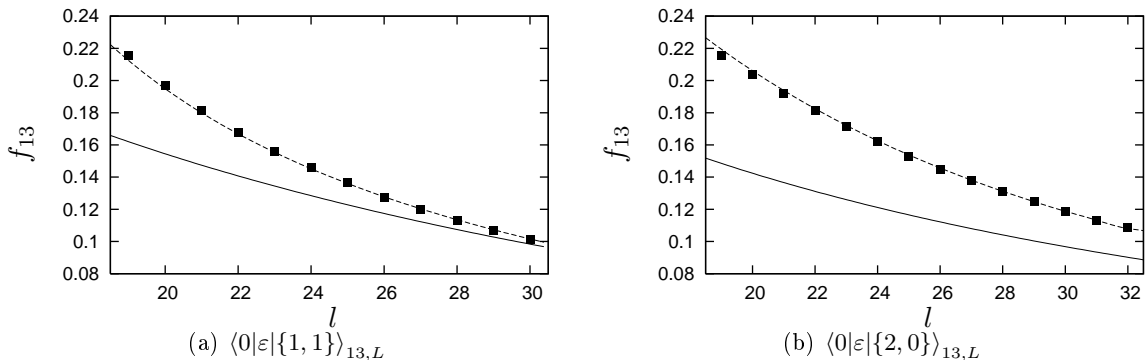


Figure 4.3: Elementary form factors of A_1A_3 scattering states, dots correspond to TCSA data. The solid lines are obtained by a “naive” evaluation of the finite volume form factors, while the dotted line represents the bound state prediction. (in this case $A_1A_1A_1$ form factors at the appropriate rapidities)

up to a physically irrelevant phase.

It is easy to show once again that the “naive” result is reproduced in the $L \rightarrow \infty$ limit. To do so, we first quote the dynamical pole equation of the infinite volume form factor:

$$F^\mathcal{O}(\theta + iu, \theta - iu, \theta_1, \dots, \theta_n)_{aab_1\dots b_n} = \frac{\Gamma_{aa}^c}{2(u - \bar{u}_{ac}^a)} F^\mathcal{O}(\theta, \theta_1, \dots, \theta_n)_{cb_1\dots b_n} + O(1)$$

The singularity of $\rho^{(n+2)}$ is given by

$$\text{Res}_{u \rightarrow \bar{u}_{ac}^a} \rho^{(n+2)}(\theta + iu, \theta - iu, \theta_1, \dots, \theta_n)_{aab_1\dots b_n} = \frac{1}{2} \rho^{(n+1)}(\theta, \theta_1, \dots, \theta_n)_{cb_1\dots b_n}$$

The “naive” formula is now recovered by inserting the last two equations into (4.8).

The leading exponential corrections can be obtained by plugging (3.7) and (3.10) into (4.8) and expanding to first order in $u - \bar{u}_{ac}^a$. This procedure is straightforward but quite lengthy, therefore we refrain from giving the details of the calculations.

In fig. 4.3 two examples are presented for the evaluation of (4.8) applied to A_1A_3 two-particle states.

5 Conclusions

In this work we determined the generalization of Lüscher’s μ -term associated to moving one-particle states, arbitrary scattering states and finite volume form factors. Our method is based on the bootstrap principle of the infinite volume theory which states that a particle which is a bound state of two others is indeed indistinguishable from the two-particle state with the appropriate (imaginary) momenta. An analytic continuation of the Bethe-Yang equations was used to quantize the bound states in finite volume.

The analytic results were tested by comparing the predictions to high-precision TCSA data of the Ising model; a satisfactory agreement was observed in each case. We also demonstrated that the bound state quantization goes beyond the leading mu-term corresponding to the fusion and gives a resummation of all powers of $e^{-\mu_{aa}^c L}$. This is a substantial improvement over the inclusion of the leading Lüscher term when other sources of finite volume corrections (other fusions, F-terms) can be neglected. Our main example was provided by particle A_3 from the E_8 scattering theory.

As an analytic check the calculations were compared to the leading order results of the exact TBA equations. The agreement between the two approaches was explicitly demonstrated in the case of the one-particle levels of the Lee-Yang model.

Our results can also be applied in nonintegrable models for states below the first inelastic threshold. However, the calculations only apply to symmetric fusions of the type $A_a A_a \rightarrow A_c$. The nonsymmetric case requires an extension of the Bethe-Yang equations to incorporate multi-channel scattering. Such a quantization scheme could also be used to describe finite volume states in nonintegrable theories above the two-particle threshold.

Acknowledgements

The author is grateful to G. Takács for his support during the completion of this work and for correcting the manuscript. The author would also like to thank Z. Bajnok for interesting discussions. This research was partially supported by the Hungarian research fund OTKA K60040.

A μ -term for the one-particle form factor

Here we develop the first order correction to (4.5). Using the exchange axiom

$$F_c^\mathcal{O}(I, L) = \frac{F^\mathcal{O}(\theta - iu, \theta + iu)_{aa}}{\sqrt{S_{aa}(-2iu)\rho_{aa}(\theta + iu, \theta - iu)}} \quad (\text{A.1})$$

The form factor axioms imply that

$$\lim_{u \rightarrow \bar{u}_{ac}^a} F^\mathcal{O}(\theta - iu, \theta + iu)_{aa} = \frac{1}{\Gamma_{aa}^c} F_c^\mathcal{O}$$

The simple pole of $\varphi_{aa}(2iu)$ in ρ_{aa} is cancelled by $S_{aa}(-2iu)$, therefore both the numerator and the denominator of (A.1) have continuous limits as $u \rightarrow \bar{u}_{ac}^a$.

The form factor $F^\mathcal{O}(\theta - iu, \theta + iu)_{aa}$ only depends on u by Lorentz-symmetry. Therefore

$$F^\mathcal{O}(\theta - iu, \theta + iu)_{aa} = \frac{1}{\Gamma_{aa}^c} F_c^\mathcal{O} - 2i (F_{aa}^\mathcal{O})' (u - \bar{u}_{ac}^a) + \dots$$

where

$$(F_{aa}^\mathcal{O})' = \frac{d}{d\theta} F^\mathcal{O}(\theta, \theta')_{aa} \Big|_{\theta - \theta' = -2i\bar{u}_{ac}^a}$$

Expanding the S-matrix element into a Laurent-series in the vicinity of the pole

$$\begin{aligned} S_{aa}(2iu) &= \frac{(\Gamma_{aa}^c)^2}{2(u - \bar{u}_{ac}^a)} + S_{aa}^{c,0} + \dots \\ S_{aa}(-2iu) &= \frac{2(u - \bar{u}_{ac}^a)}{(\Gamma_{aa}^c)^2} - \left(\frac{2(u - \bar{u}_{ac}^a)}{(\Gamma_{aa}^c)^2} \right)^2 S_{aa}^{c,0} + \dots \end{aligned}$$

Expanding the denominator:

$$\begin{aligned} S(-2iu)\rho_{aa}(\theta + iu, \theta - iu) &= \\ S(-2iu)E_1 E_2 L^2 - i(E_1 + E_2)L S'(2iu) \left(S(-2iu) \right)^2 &= \\ \frac{E_c L}{(\Gamma_{aa}^c)^2} + \left(\frac{2E_1 E_2 L^2}{(\Gamma_{aa}^c)^2} - \frac{4E_c L}{(\Gamma_{aa}^c)^4} S_{aa}^{c,0} \right) (u - \bar{u}_{ac}^a) + \dots \end{aligned}$$

where

$$E_c = E_1 + E_2 = 2m_a \cos(u) \cosh(\theta)$$

Putting all this together

$$\begin{aligned} F_c^\mathcal{O}(I, L) &= \frac{F_c^\mathcal{O}}{\sqrt{E_c L}} + \\ &+ \left[\frac{-2i\Gamma_{aa}^c (F_{aa}^\mathcal{O})'}{\sqrt{E_c L}} + \frac{F_c^\mathcal{O}}{\sqrt{E_c L}^3} \left(-E_1 E_2 L^2 + \frac{2E_c L}{(\Gamma_{aa}^c)^2} S_{aa}^{c,0} \right) \right] (u - \bar{u}_{ac}^a) + \dots \end{aligned}$$

Note that in the preceding formulas E_c does include the leading order correction to the usual one-particle energy $E_c^0 = \sqrt{m_c^2 + (2\pi I)^2/L^2}$. Using

$$E_c = E_c^0 - 2\frac{m_c\mu}{E_c^0}(u - \bar{u}_{ac}^a) + O(e^{-2\mu L}) \quad \text{and} \quad E_1 E_2 = \frac{m_a^2}{m_c^2} E_c^2 - \mu^2$$

the final result is given by

$$\begin{aligned} F_c^{\mathcal{O}}(I, L) &= \frac{F_c^{\mathcal{O}}}{\sqrt{E_c^0 L}} - \frac{2i\Gamma_{aa}^c (F_{aa}^{\mathcal{O}})'}{\sqrt{E_c^0 L}}(u - \bar{u}_{ac}^a) + \\ &+ \frac{F_c^{\mathcal{O}}}{\sqrt{E_c^0 L}} \left[\frac{2S_{aa}^{c,0}}{(\Gamma_{aa}^c)^2} + \frac{m_c\mu}{(E_c^0)^2} - \left(\frac{m_a^2}{m_c^2} E_c^0 - \frac{\mu^2}{E_c^0} \right) L \right] (u - \bar{u}_{ac}^a) + O(e^{-2\mu L}) \end{aligned} \quad (\text{A.2})$$

with

$$u - \bar{u}_{ac}^a = \pm \frac{1}{2} (\Gamma_{aa}^c)^2 e^{-\mu_{aa}^c L} \sqrt{1 + \left(\frac{\pi I}{m_a L \cos(\bar{u}_{ac}^a)} \right)^2}$$

References

- [1] M. Lüscher, *Commun.Math.Phys.* **105** (1986) 153-188.
- [2] M. Lüscher and U. Wolff, *Nucl.Phys.* **B339** (1990) 222-252.
- [3] M. Lüscher, *Nucl.Phys.* **B364** (1991) 237-254.
- [4] B. Pozsgay and G. Takács, *Nucl.Phys.* **B748** (2006) 485-523. [hep-th/0604022](#)
- [5] M. Lüscher, *Commun.Math.Phys.* **104** (1986) 177.
- [6] T.R. Klassen and E. Melzer, *Nucl. Phys.* **B362** (1991) 329-388.
- [7] R. Janik and T. Lukowski, *Phys.Rev.* **D76** (2007) 126008, [arXiv:0708.2208](#) [[hep-th](#)]
- [8] M. Heller, R. Janik and T. Lukowski, [arXiv:0801.4463](#) [[hep-th](#)]
- [9] B. Pozsgay and G. Takács, *Nucl.Phys.* **B788** (2008) 209-251. [arXiv:0706.3605](#) [[hep-th](#)]
- [10] L. Lellouch, M. Lüscher, *Commun.Math.Phys.* **219** (2001) 31-44.
- [11] C.-J.D. Lin, G. Martinelli, C.T. Sachrajda, M. Testa, *Nucl.Phys.* **B619** (2001) 467-498.
- [12] B. Pozsgay and G. Takács, *Nucl.Phys.* **B788** (2008) 167-208. [arXiv:0706.1445](#) [[hep-th](#)]
- [13] V.P. Yurov and A.I.B. Zamolodchikov, *Int.J.Mod.Phys.* **A6** (1991) 3419-3440.
- [14] H. Kausch, G. Takács and G. Watts, *Nucl.Phys.*, **B547** (1999) 538-568. [hep-th/9605104](#)
- [15] Z. Bajnok, L. Palla and G. Takács, *Nucl.Phys.* **B614** (2001) 405-448. [hep-th/0106069](#)
- [16] P. Dorey and R. Tateo, *Nucl.Phys.* **B482**, (1996) 639-659. [hep-th/9607167](#)
- [17] A.B. Zamolodchikov, *Int.J.Mod.Phys.* **A4** (1989) 4235.
- [18] V.P. Yurov and A.I.B. Zamolodchikov, *Int.J.Mod.Phys.* **A6** (1991) 4557-4578.
- [19] Z. Bajnok, L. Palla, G. Takács and F. Wágner, *Nucl. Phys.* **B587** (2000) 585-618. [hep-th/0004181](#)
- [20] Z. Bajnok, L. Palla and G. Takács, *Nucl.Phys.* **B702** (2004) 448-480. [hep-th/0406149](#)
- [21] L. Maiani, M. Testa, *Phys.Lett.* **B245** (1990) 585-590.
- [22] G. Delfino and P. Simonetti, *Phys.Lett.* **B383** (1996) 450-456. [hep-th/9605065](#)
- [23] G. Delfino, P. Grinza and G. Mussardo, *Nucl.Phys.* **B737** (2006) 291-303. [hep-th/0507133](#)

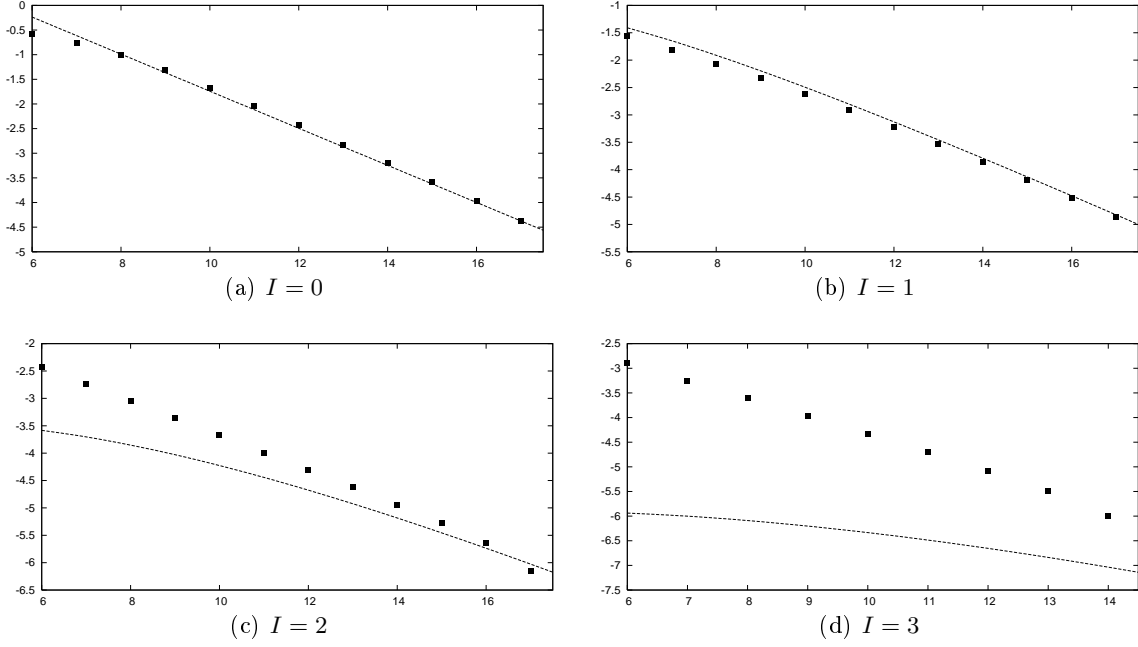


Figure A.1: Finite size corrections to A_1 one-particle levels in sectors $I = 0 \dots 3$, $\log_{10}\Delta e$ is plotted as a function of the volume. Dots represent TCSA data, while the lines show the μ -term corresponding to the $A_1 A_1 \rightarrow A_1$ fusion.

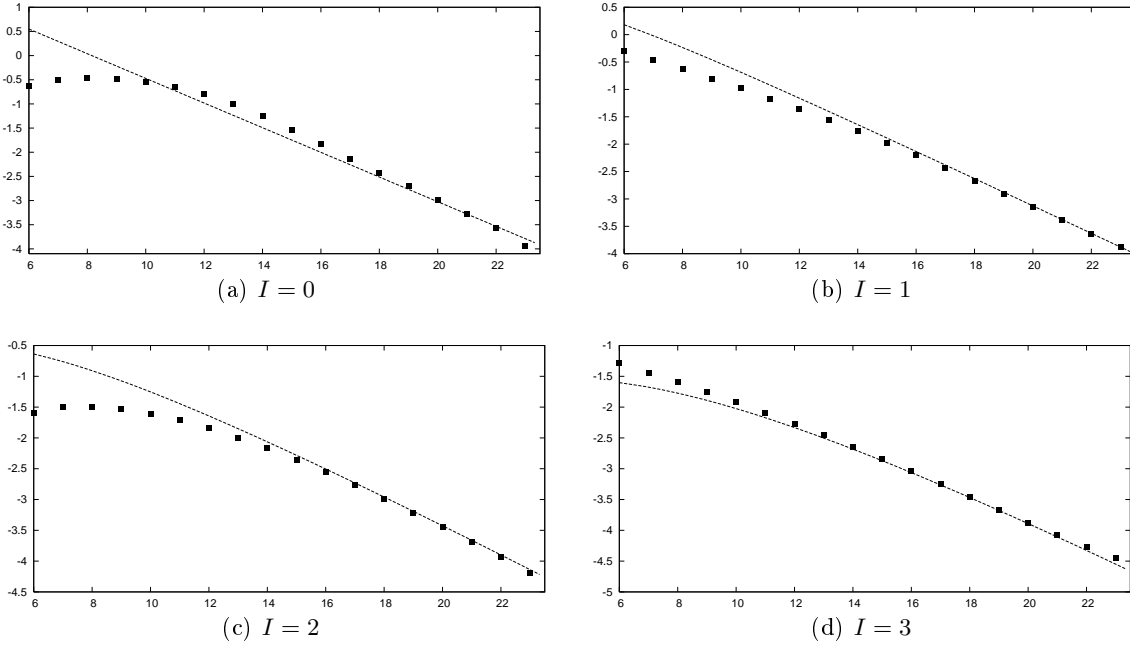


Figure A.2: Finite size corrections to A_2 one-particle levels in sectors $I = 0 \dots 3$, $\log_{10}\Delta e$ is plotted as a function of the volume. Dots represent TCSA data, while the lines show the μ -term corresponding to the $A_1 A_1 \rightarrow A_2$ fusion.

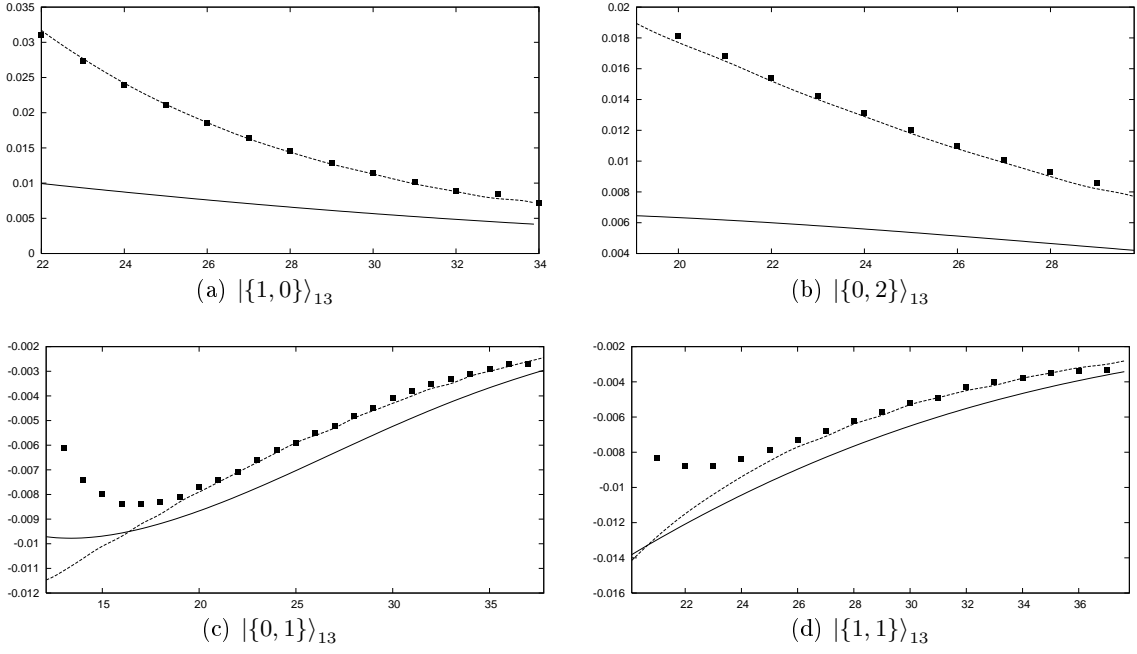


Figure A.3: Finite size corrections to A_1A_3 scattering states as a function of the volume. Dots represent TCSA data, the solid line shows the μ -term corresponding to the $A_1A_1 \rightarrow A_3$ fusion. The dotted lines are obtained by the exact solution of the quantization condition for the $A_1A_1A_1$ three-particle system.

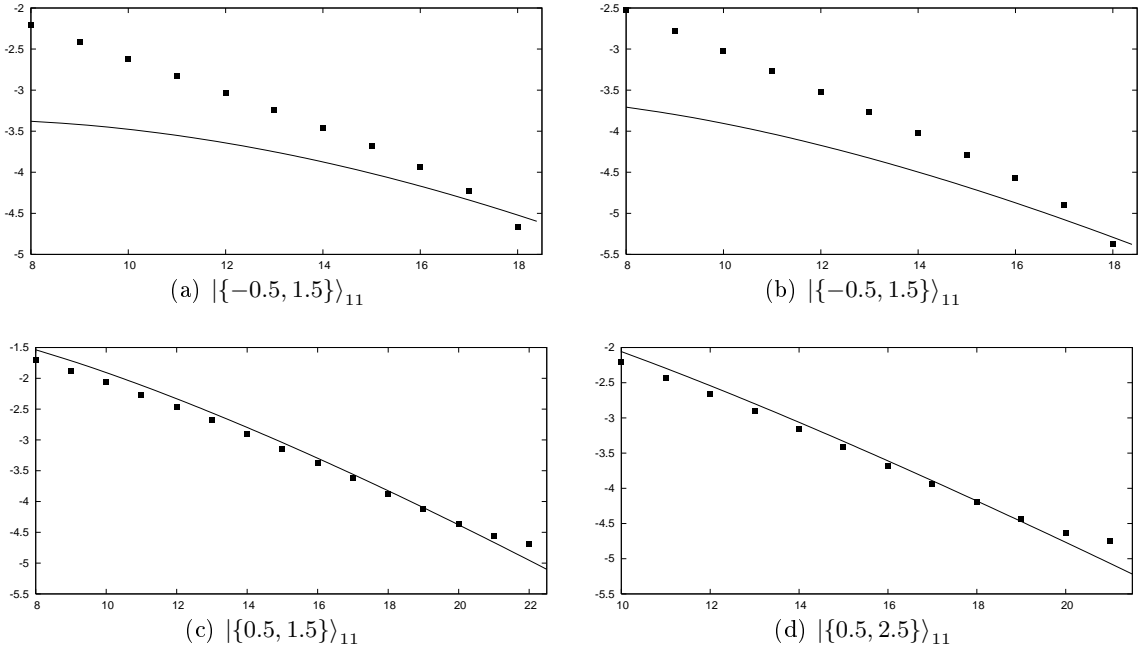


Figure A.4: Finite size corrections to A_1A_1 scattering states, $\log_{10}\Delta e$ is plotted as a function of the volume. Dots represent TCSA data, while the solid line show the sum of the two μ -terms corresponding to the $A_1A_1 \rightarrow A_1$ fusions.

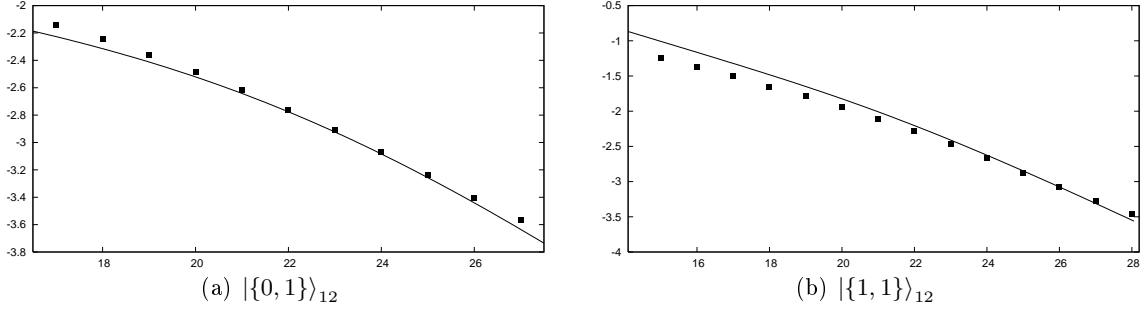


Figure A.5: Finite size corrections to A_1A_2 scattering states, $\log_{10}\Delta e$ is plotted as a function of the volume. Dots represent TCSA data, while the solid line show the μ -term corresponding to the $A_1A_1 \rightarrow A_2$ fusion.

l	θ_1	θ_2	θ_3	$e(l)$ (predicted)	$e(l)$ (TCSA)
22	0.44191	0.68235	-0.58742	3.51877	3.51900
23	0.42574	0.64280	-0.55190	3.46201	3.46219
24	0.60523	0.41155	-0.51892	3.41239	3.41255
25	0.56934	0.39931	-0.48831	3.36890	3.36907
26	0.38910	0.53475	-0.45989	3.33071	3.33089
27	0.50092	0.38119	-0.43350	3.29709	3.29729
28	0.46686	0.37634	-0.40899	3.26743	3.26767
29	0.42947	0.37739	-0.38622	3.24122	3.24164
30	$0.38646 + 0.02332 i$	$0.38646 - 0.02332 i$	-0.36505	3.21801	3.21832
31	$0.37059 + 0.04042 i$	$0.37059 - 0.04042 i$	-0.34537	3.19741	3.19775
32	$0.35572 + 0.05104 i$	$0.35575 - 0.05104 i$	-0.32706	3.17908	3.17945
33	$0.34182 + 0.05891 i$	$0.34182 - 0.05891 i$	-0.31002	3.16275	3.16313
34	$0.32876 + 0.06513 i$	$0.32876 - 0.06513 i$	-0.29415	3.14816	3.14856
35	$0.31650 + 0.07022 i$	$0.31650 - 0.07022 i$	-0.27936	3.13511	3.13547
36	$0.30498 + 0.07446 i$	$0.30498 - 0.07446 i$	-0.26556	3.12341	3.12235

Table A.1: An example for the dissociation of the A_1A_1 bound state inside a scattering state. $|\{2,0\}\rangle_{31,L}$ is identified with $|\{1,1,0\}\rangle_{111,L}$ and the corresponding Bethe-Yang equations is solved. For $l < 30$ there is a real $A_1A_1A_1$ three-particle state in the spectrum, whereas at $l \approx 30$ two of the rapidities become complex and the two-particle state A_1A_3 emerges.

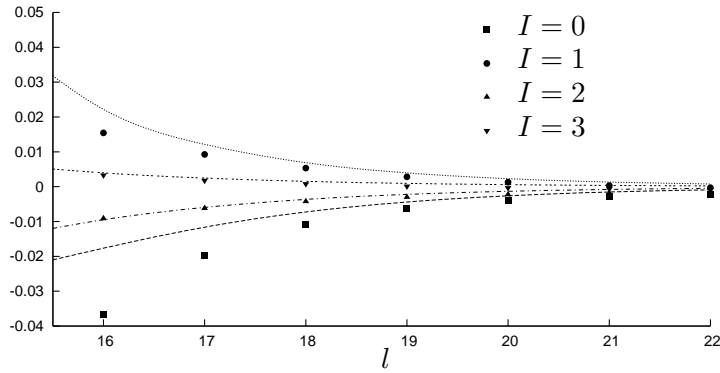


Figure A.6: Finite size corrections to the elementary form factors of A_2 . Dots represent TCSA data, while the lines show the μ -term prediction corresponding to the $A_1A_1 \rightarrow A_2$ fusion.